JOC The Journal of Organic Chemistry

Article

pubs.acs.org/joc

Mechanistic and Sterochemical Insights on the Pt-Catalyzed Rearrangement of Oxiranylpropargylic Esters to Cyclopentenones

Adán B. González-Pérez, Belén Vaz, Olalla Nieto Faza,* and Ángel R. de Lera*

Departamento de Química Orgánica, Facultade de Química, Universidade de Vigo, 36310 Vigo, Spain.

Supporting Information

ABSTRACT: A mechanism for the rearrangement of oxiranylpropargylic esters to cyclopentenones catalyzed by $PtCl_2$ is proposed based on DFT calculations (M06/6-31++G(d,p)). Although the basic steps are coincidental with those proposed by Sarpong et al., who characterized a 2*H*-pyran as intermediate, calculations have revealed other intricate details of this complex rearrangement. The 2*H*-pyran is proposed to result from the ring-opening of a bicyclic oxonium ion that follows the nucleophilic capture by the epoxide of a platinum carbene generated by an initial Pt-mediated 1,2-propargylic rearrangement. The key steps in the evolution of this system are the electrocyclic ring-opening of the 2*H*-pyran to a α-methoxycarbonyl dienone and an iso-Nazarov ring closure. Prior to those, changes in hapticity and in the conformation of the dienone are required in order to produce the helical conformation needed to generate a single diastereomer of the cyclopentenone product obtained experimentally. The metal is needed well beyond the first step of the mechanism, and both electrocyclic reactions are favored by coordination to the metal when compared to their uncomplexed counterparts. Moreover, we have experimentally demonstrated that the rearrangement is stereoconvergent, a feature that is traced back to the initial configuration of the epoxide, which determines the somewhat counterthermodynamic placement of the metal *syn* to the methyl group of the stereogenic center in the 2*H*-pyran intermediate. Finally, starting from enantiopure oxiranylpropargylic ester **13**, a racemate of cyclopentenone (*R**,*S**)-**16** was obtained. Thus, the sequence does not proceed with memory of chirality, and the absolute stereochemical information is already lost at the stage of the 2*H*-pyran **14**.

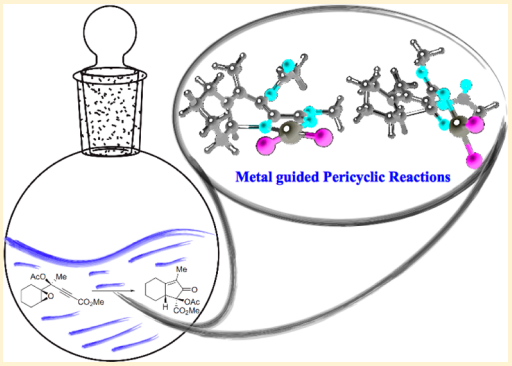

INTRODUCTION

The use of gold and platinum complexes in homogeneous catalysis has experienced an unprecedented development in the past decade. These new synthetic tools exploit the properties of noble metals as activators of carbon−carbon π-bonds functioning as soft, carbophilic Lewis acids in reactions that achieve a large increase in molecular complexity under mild conditions, compatible with a wide range of functional groups.[1−14] In particular, their application as catalysts in intramolecular skeletal rearrangements has captured the interest of chemists through the provision of an efficient and atom-economical method of generating cyclic compounds with complex structures and a defined configuration.

Propargylic esters have been one of the most studied substrates for reactions with gold or platinum,[15] since they are easily available, can be densely functionalized, and offer the possibility of an initial 1,2- or 1,3-ester migration that opens the way to a rich catalytic manifold involving different paradigms of reactivity, resulting in interesting intramolecular rearrangements.[16−19] The dual role of the catalyst in this environment rich in functional groups, as both a simple alkynophilic Lewis acid and an organizing metallic center has been proposed and exploited in a large number of recent contributions.[4,20−25] Upon activation of the alkyne by coordination to the metal, the intramolecular nucleophilic attack of the carbonyl in the carboxylate moiety can occur at either termini of the insaturation, and this is followed by the propargylic C−O bond cleavage, which completes the 1,2- or 1,3-ester migration. The barriers for these potentially reversible processes are usually low, and the preference for one or another will depend on the functionalization of the reactant and the further evolution of the allene or carbenoid/carbocationic intermediate thus generated.[26] The most common evolution of this allene or carbenoid or cationic species[1,26−29] is by nucleophilic attack of an external or internal nucleophile.

When the internal nucleophile is an olefin (an *1,n*-enyne as a reactant),[4,6,30,31] the alkyne-metal complex usually reacts with the alkene to yield exo or endo cyclopropyl carbenes through either a 5-exo-dig or a 6-endo-dig cyclization, respectively, that can further evolve following different rearrangement patterns. In the presence of other nucleophiles, alternative adducts can be formed, and more complex transformations can be achieved starting from more functionalized enynes.[32] This is the case when the alkene is replaced by an oxirane,[33,34] or an aziridine,[35] opening new mechanistic possibilities. Sarpong et al. recently reported an impressive one-pot transformation of oxiranyl propargylic esters such as **i** to 2-cyclopentenones **iii** catalyzed by $PtCl_2$ which occurs with high regio- and diastereoselectivity (see Scheme 1).[36]

Received: August 13, 2012
Published: September 10, 2012

dx.doi.org/10.1021/jo301651r | J. Org. Chem. 2012, 77, 8733−8743

Scheme 1[a]

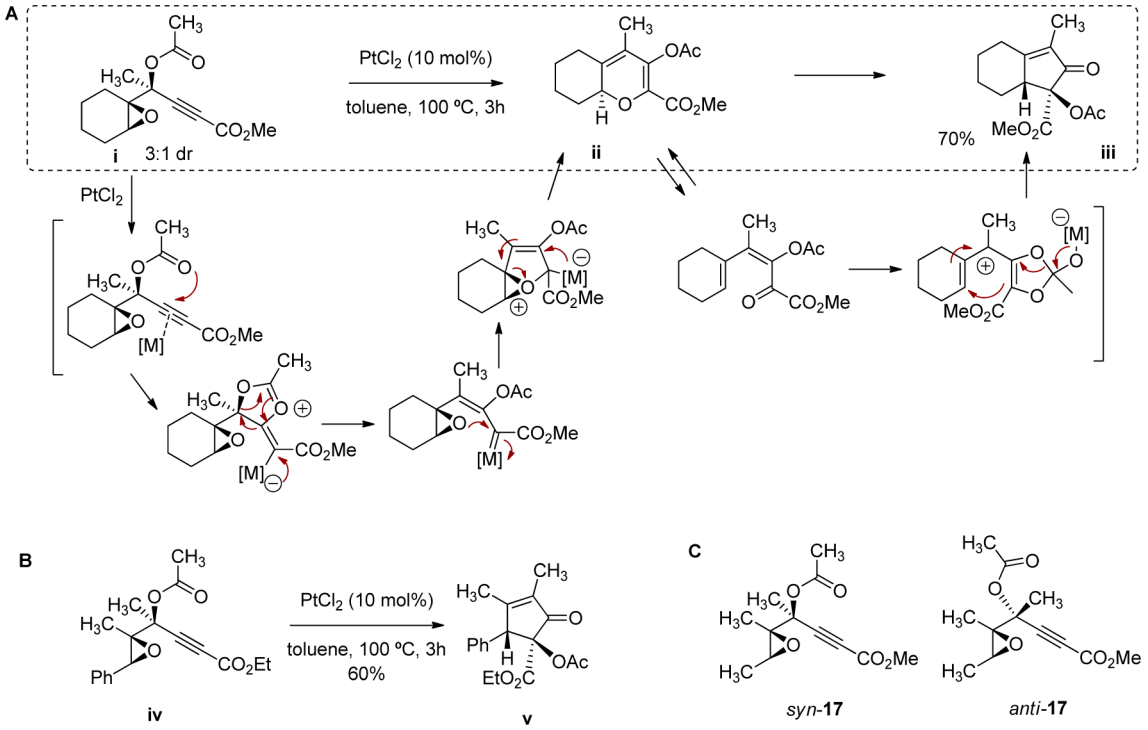

[a]A. General reaction mechanism proposed for the pentannulation of oxiranyl propargylic esters. A substituted 2*H*-pyran (**ii**) was isolated as an intermediate in this transformation under modified conditions (in the presence of 20 mol % COD).[36] B. Rearrangement of the acyclic analogue **iv** to **v**. C. Model system (**17**) for the computational studies on the rearrangement of **iv**.

Our previous study of another noble metal catalyzed propargylic ester rearrangement,[33] with an internal epoxide as a nucleophile,[37] prompted our interest in this complex transformation. The challenge involved in explaining the mechanism of this rearrangement (4 covalent bonds are broken/formed in a single experimental step) and the diastereoselectivity of the transformation fueled this interest to computationally explore the evolution of the proposed intermediates[20] in such a densely functionalized substrate. Also of interest is the transfer of chiral information from the epoxide in **i** (both diastereoisomers were used) to cyclopentenone **iii**. At the outset, the process can be considered stereoconvergent as both *syn* and *anti* diastereomers led to the same product of relative configuration (*R**,*S**). Furthermore, although starting epoxyesters were used as racemates, the possibility of a transfer of chiral information from enantiopure substrates needs to be examined as well. The latter stereochemical feature has been described in the rearrangement of enantiopure propargylic alcohols with noble metals in similar settings and found, through computational studies, to be justified by the intermediacy of enantiopure helically chiral intermediates.[21,38]

As a starting point, we used the mechanism proposed by Sarpong,[36] which proceeds through the formation of a 2*H*-pyran intermediate **ii** that undergoes an oxa-6π electrocyclic ring-opening to a functionalized dienone, which is transformed on its turn into the product **iii** through a ring closure and an associated acyl shift. The intermediacy of **ii** was confirmed in one case, when 1,5-cyclooctadiene (20 mol %) was added together with $PtCl_2$. Acyclic epoxyesters such as **iv** (Scheme 1B) were also valid substrates in the precedent experimental work,[36] and they were shown to undergo an analogous rearrangement to produce a single diastereomer of **v**.

The Results and Discussion section will be organized according to the following studies: (1) computations on the rearrangement of reactant **i** to cyclopentenone (*R*,*S*)-**iii**; (2) experimental studies on the memory of chirality using enantiopure substrates; (3) experimental and computational studies on the stereoconvergent nature of the rearrangement of acyclic system **iv**. For the theoretical part in the last section, the acyclic analog methyl (*S*)-4-acetoxy-4-((2*R*,3*S*)-2,3-dimethyloxiran-2-yl)pent-2-ynoate (*syn*-**17**) and its diastereoisomer (*anti*-**17**) were chosen as simplified models on which further mechanistic possibilities differing in the coordination modes of Pt were addressed, what allowed to demonstrate an additional level of selectivity (torquoselectivity) with these substrates.

METHODS

DFT calculations with the hybrid meta GGA functional M06, which has shown good performance in transition metal-catalyzed reactions,[39,40] and also specifically in gold-catalyzed rearrangements,[15,41] have been carried out using *Gaussian09*[42] to locate and characterize the stationary points on the potential energy surface. The 6-31++G(d,p) basis set has been used for the main group elements, while the LANL2DZ basis set,[43] in which the innermost electrons are replaced by an ECP and the valence electrons are explicitly treated by a double-ζ basis set, has been applied to Pt. The optimized geometries have been characterized by harmonic analysis, and the nature of the stationary points determined according to the number of negative eigenvalues of the Hessian matrix. In several doubtful cases, internal reaction coordinates (IRCs) have been followed from the transition structures to verify the proper connections with reactants and products.[44] Zero-point vibration energies (ZPVE) and thermal corrections (at 298 K, 1 atm) to the energy have been estimated using the computed frequencies applying the free particle, harmonic oscillator, and rigid rotor approximations at the high temperature limit in a canonical ensemble. Solvation effects (to simulate the experimentally used

dx.doi.org/10.1021/jo301651r | J. Org. Chem. 2012, 77, 8733−8743

toluene solvent) have been also included as single point corrections to the gas-phase free energy of the optimized structures with the self-consistent reaction field (SCRF) method using the polarizable continuum model (PCM)[45,46] as implemented in *Gaussian09*. The energetic span model has been used to compute the energy difference defined by the TDI (turnover frequency determining intermediate) and TDTS (turnover frequency determining transition state) using *AUTOF*.[47−49] Figures 1 and 2 were prepared using *CYLView*.[50]

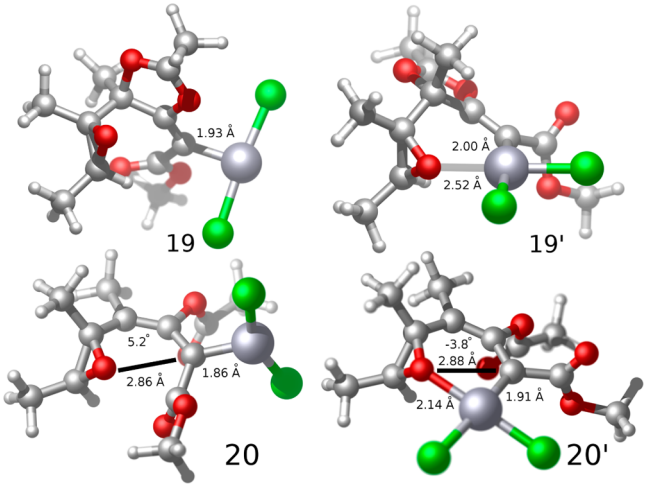

Figure 1. Representation of the platinum carbenoid intermediates **20** and **20′** starting from the *syn* and *anti* diastereomers of epoxypropargylic ester **17** via **19** and **19′**. Bond distances are given in Å and dihedral angles in degrees for the structures calculated at the M06/6-31++G(d,p) level in toluene (PCM).

General experimental methods and structural characterization of the products depicted in Scheme 5 can be found as Supporting Information.

RESULTS AND DISCUSSION

Mechanistic Insights into the Rearrangement of Diastereomer *syn*-i. The electronic structure calculations of the different steps involved in the rearrangement of model system methyl (*S*)-4-acetoxy-4-((1*R*,6*S*)-7-oxabicyclo[4.1.0]-heptan-1-yl)pent-2-ynoate (*S*,*R*,*S*)-**i** (*syn*-**i**) led to the general proposal depicted in Scheme 2. Choosing arbitrarily one of the enantiomers would allow us to investigate the transfer of

Scheme 2. General Mechanistic Proposal for the the $PtCl_2$-Promoted Pentannulation of Model Oxiranyl Propargylic Ester *syn*-i of (*S*,*R*,*S*) Configuration to Cyclopentenone (*R*,*S*)-iii[a]

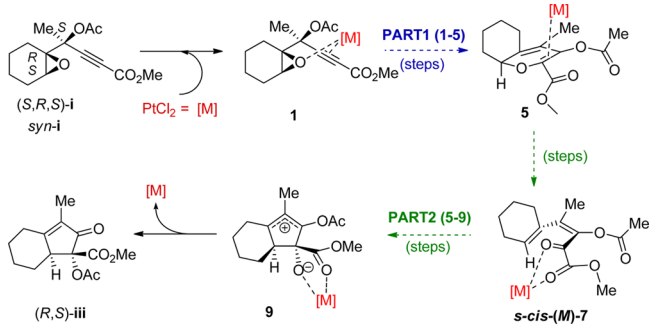

[a]A more detailed description of its different sections will be provided along the discussion.

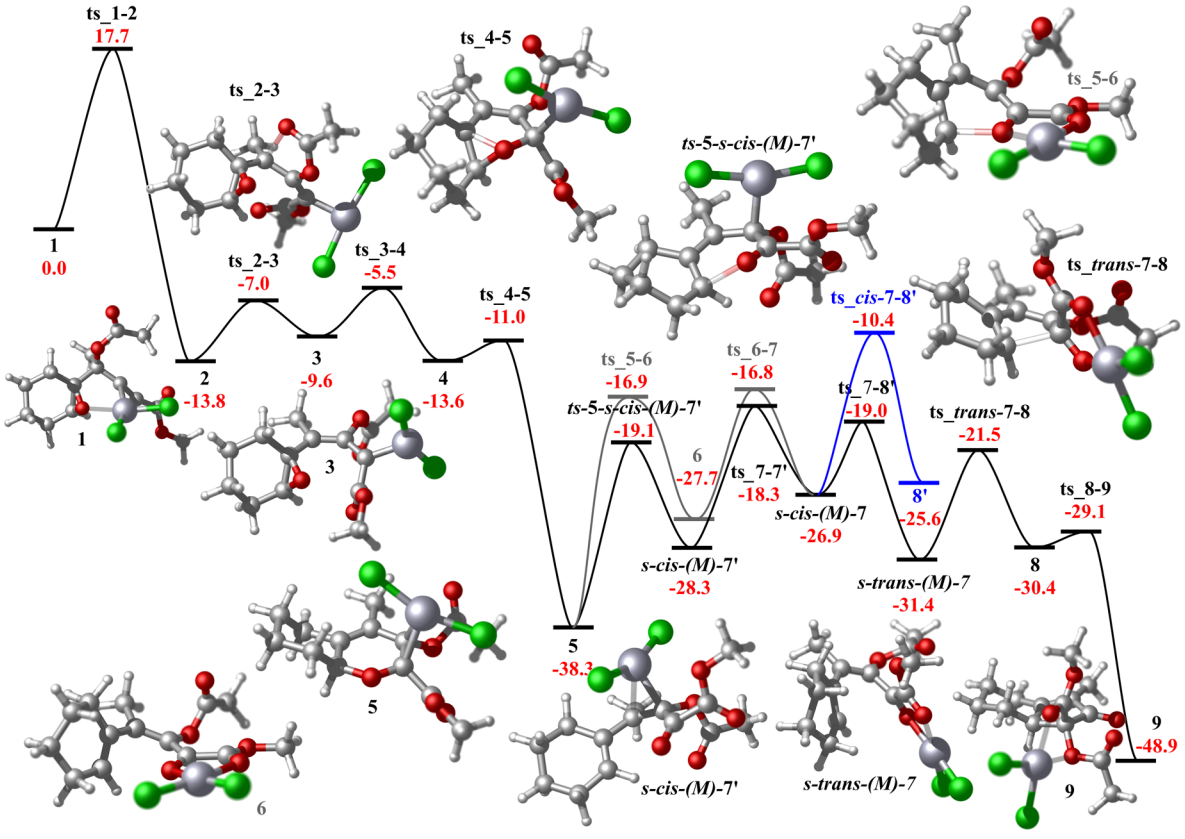

Figure 2. Free energy profile for the $PtCl_2$ catalyzed cycloisomerization of **i**. Activation free energies in kcal/mol are indicated over the arrows connecting the intermediates. Structures and energies have been computed at the M06/6-31++G(d,p) level in toluene (PCM).

dx.doi.org/10.1021/jo301651r | *J. Org. Chem.* 2012, 77, 8733−8743

chirality to the final product and predict the major enantiomer in case the system preserves the "memory of chirality".[51]

Besides the uncommonly large number of steps for a one-pot cascade transformation, two features immediately stand out from the scheme in Scheme 2: first, the changing role of the catalyst and its multiple coordination possibilities in a delicate interplay between functional groups and, second, the apparent loss and ulterior recovery of chirality.

For simplicity, we have split the general mechanism in Scheme 2 into two sections, each dominated by a step that is key to the evolution of the system, either in terms of the formation of a critical bond or in terms of transfer of chiral information. The first section deals with the transformation of *syn*-**i** into dihydropyran **5**, the only intermediate that could be isolated in the experiment, through a mechanism that essentially agrees with Sarpong's original proposal (Scheme 1).[36] In the second, the evolution of **5** to **7** and then to cyclopentenone **9** is studied. Although no large alterations of the molecular skeleton are involved in it, this part of the mechanism is key to rationalizing how chirality transfer might be attained through formally achiral intermediates, such as the dienone product **7**. A series of metal migrations and conformational changes with non-negligible energy barriers, together with an electrocyclic ring-opening, and a platinum-catalyzed iso-Nazarov four-electron electrocyclization are proposed in this part. With the defined configurations at C_2 and C_3 of the final product established after these steps, the reaction product is finally formed by acetate migration in **9** and the final cyclopentenone (*R*,*S*)-**iii** is obtained after detachment of the $PtCl_2$ catalyst.

Part 1. The reaction sequence starts with the formation of a π complex (**1**) between $PtCl_2$ and *syn*-**i** where platinum is coordinated to the alkyne and to the oxirane (Scheme 3).

Scheme 3. Activation of the Acetoxy Propargyloxirane by $PtCl_2$ and Subsequent Transformation into 5[a]

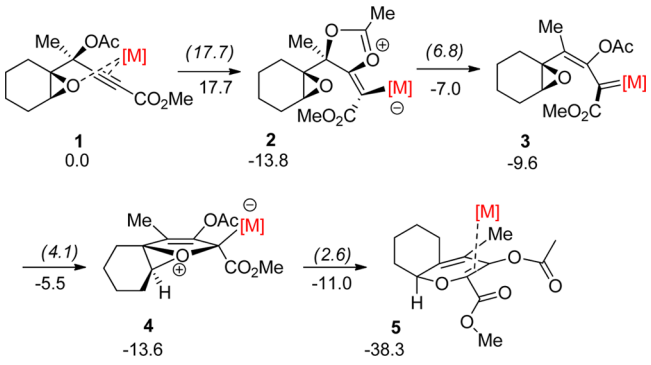

[a]Relative and activation (*in parentheses*) free energies in kcal/mol have been computed at the M06/6-31++G(d,p) level in toluene (PCM).

Following a reactivity scheme quite common for this kind of gold or platinum-activated propargyl esters,[15−19] **1** evolves through 1,2-acetate migration via intermediate **2** to structure **3** with T geometry around the metal center. In the carbene−carbocation continuum found for these kind of intermediates, this species is better considered as a platinum carbenoid,[1,27−29] judging from the Pt−C bond distance (1.869 Å) which is in line with those measured in crystal structures of platinum carbenes[52,53] and in related species characterized computationally.[54] The oxirane oxygen and the platinum atom are coordinated in the nearly planar structure **3** (see Figure 1 for its acyclic counterparts). This platinum carbene intermediate then undergoes intramolecular nucleophilic capture by the oxirane to form the highly congested bicyclic dihydrofuran oxonium ion **4**, through a rotation of the platinum to the β-face coupled to the formation of the C−O bond (for a relaxed scan of this coordinate, see Supporting Information). Compound **4** on its turn experiences a facile (about 3 kcal/mol) fragmentation/ring expansion to afford the platinum-coordinated 2*H*-pyran **5**.

In our studies on the gold-catalyzed rearrangement of the related (3-acyloxyprop-1-ynyl)oxiranes, the metal coordinated only one of the two functionalities (alkyne or oxirane) present in the reactant.[37] It is the proximity of the two functions in substrate **i** together with the avidity of the metal to form complexes (with unsaturations or heteroatom lone pairs) what induces the bidentate coordination of platinum, and this in turn determines the configuration of the complexes in the ensuing events. Thus, 1,2-acetate migration occurs *syn* to the coordinated platinum to afford **2** and subsequently a series of intermediates in which the configuration of the proximal stereogenic center of the epoxide is transferred to the metal-containing stereocenter in **4** and then to the planar chirality of the 2*H*-pyran **5** formed upon ring-opening of **4**.

Part 2. The second part of the mechanism revolves around an electrocyclic ring-opening followed by an iso-Nazarov cyclization (Scheme 4). The transformation of **5** into **7** (the *M* enantiomer starting from the configuration of the epoxide arbitrarily chosen in **1**) is formally an electrocyclic ring-opening. On the basis of our computations, a conformational change and metal migration step with non-negligible barriers are proposed to take place prior to the ring-opening to form complex **6** (Scheme 4). This step (**ts5−6**) involves a rotation of the ester group associated to a displacement of the metal center on the β plane to form a bidentate complex with platinum coordinated to the oxygen atoms of the carboxyl group and the 2*H*-pyran ring. The result of this metal migration (**6** is destabilized relative to **5** by 10.6 kcal/mol), which shows a rather high barrier for a nonreactive step (21.4 kcal/mol), is a net conformational change leading to a displacement of the pyran oxygen from the heterocycle plane. The coordination of the metal to both O lone pairs and the enhanced sp^3 character of the ring oxygen in **6** forces the hydrogen of the remaining stereogenic center to adopt a pseudoaxial orientation. The subsequent electrocyclic ring-opening of the 2*H*-pyran complex **6** has an activation energy of 10.9 kcal/mol and affords *s-cis* dienone (*M*)-**7** with *M* helicity as its only product. The helicity is controlled by the torquoselective conrotation, itself determined by the stereogenic center in **6** and the greater destabilization of the alternative conrotatory mode which would place the cyclohexene facing the ketone.

As depicted in Scheme 4, both **5** (with Pt coordinated to the alkene) and its haptomer **6** (with Pt coordinated to oxygens) can undergo an electrocyclic ring-opening to yield a hexadienone structure, but this process needs to be accompanied by migration of the Pt center from the carbon backbone to the oxygens in the periphery to provide the structure required for the next step in the mechanism (an iso-Nazarov cyclization). The electrocyclic ring-opening is 8.3 kcal/mol more favorable in **6** than in **5**; however, Pt migration is more favorable on the hexadienone s-cis(*M*)-**7′** (product of the opening of **5**) than on **5** itself (10 vs 21 kcal/mol), pointing toward 5-s-cis(*M*)-**7**−s-cis(*M*)-**7** as the preferred path for this sequence of steps.

As suggested by the high activation energy (16.5 kcal/mol) (Table S1, Scheme 4) for the cyclization of *s-cis*-(*M*)-**7**, this structure is not an appropriate substrate for the next step in

dx.doi.org/10.1021/jo301651r | J. Org. Chem. 2012, 77, 8733−8743

Scheme 4. Sequence of Metal Migration, Electrocyclic Ring-Opening, and Conformational Change for the Transformation of 5 into *s-trans*-(*M*)-7, and iso-Nazarov Electrocyclic Ring Closures after Conformational Change in 7, and Acetyl Migration in 8[a]

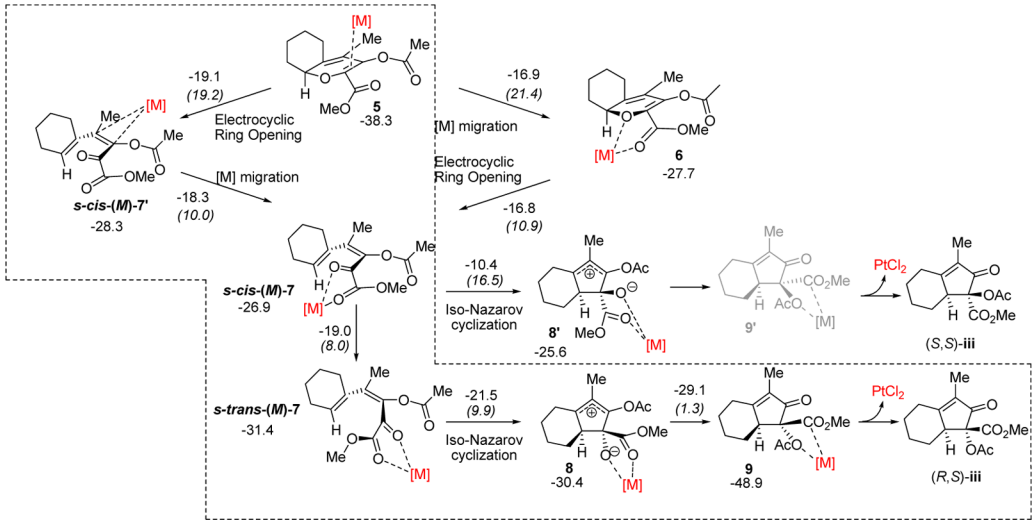

[a]A platinum migration on the 2*H*-pyran structure facilitates the electrocyclic ring-opening from **6** to **7**. Relative and activation (*in parentheses*) free energies (in kcal/mol) have been computed at the M06/6-31++G(d,p) level in toluene (PCM).

the mechanism. Moreover, this would lead to diastereomer (*S*,*S*)-**iii** contrary to the experimental findings. The iso-Nazarov electrocyclization[55,56] starts instead from *s-trans*-(*M*)-**7**, which is generated from the former by an additional conformational change along the carbonyl-Cα ester bond. The facile (9.9 kcal/mol) iso-Nazarov ring closure of *s-trans*-(*M*)-**7**, where platinum can act as a Lewis acid activating the conjugated system,[57−59] leads to the formation of cyclopentenyl cation **8** through a torquoselective four-electron electrocyclic ring-closure, which sets the configuration of the two stereocenters in the product (*R*,*S*)-**iii**. The torquoselectivity is determined by the helicity of *s-trans*-(*M*)-**7**,[21,38] which makes only one of the two Woodward−Hoffmann allowed conrotations feasible. This additional level of selectivity would ensure that the chiral information from the original oxirane previously preserved in the stereocenter and the metal orientation on the 2*H*-pyran intermediate **5** would be transferred to the cyclopentenone (*R*,*S*)-**iii**. After this step, nucleophilic attack of the platinum-stabilized alkoxy group to the acetate carbonyl is very favorable (1.3 kcal/mol) and results in acetyl migration and formation of cyclopentenone **9**, which affords product (*R*,*S*)-**iii** upon detachment of the $PtCl_2$ catalyst.

Due to the large number of coordination possibilities of the metal to the different functional groups, a detailed analysis of the two pericyclic reactions was deemed compulsory. In order to carry out a comprehensive study of the alternative Iso-Nazarov cyclizations, the acyclic analogue of **5** was selected as a model structure. In addition to answering some of the questions related to the general mechanism outlined above, this substrate allows us to address the additional possibility of formation of *Z* isomers of the hexadienone structures and its consequence on the stereoselectivity. This study is presented at the end of this paper (see Scheme 7).

On the Transfer of Chirality of the $PtCl_2$-Catalyzed Rearrangement of Oxiranyl Propargylic Esters. Although this issue was not addressed in the original disclosure by Sarpong et al.[36], the computationally based mechanism leaves open the possibility of the transfer of stereochemical information from the stereocenters of the substrate to those of the cyclopentenone via chiral nonracemic helical intermediates, as we have computationally shown[21] for the gold-catalyzed Rautenstrauch rearrangement.

In order to demonstrate whether the reaction shows memory of chirality, we prepared enantiopure propargylacetates *syn*-**13** and *anti*-**13** (see Scheme 5) from the reaction of previously described epoxyaldehyde **10**[60] and the anion (LHMDS, THF, −78 °C) of methylpropiolate **11** (38:62 *syn*-**12**/*anti*-**12**; 83%) followed by acetylation of each separated diastereomer (Ac_2O, Et_3N, DMAP, CH_2Cl_2; 90% for *syn*-**13** and 78% for *anti*-**13**). The structure of *syn*-**12** was secured by X-ray analysis (see Supporting Information).

When a solution of *anti*-**13** was heated in the presence of $PtCl_2$ (10 mol %) at 100 °C for 1.5 h, a mixture containing 2*H*-pyran **14** (53%) and furan **15** (28%) was obtained (Scheme 5). Isolated 2*H*-pyran **14** was further treated under the same conditions for 6 h, which produced cyclopentenone **16** in 75% yield. The X-ray structure of this enone revealed it to be a racemic compound, since both enantiomers are present in the crystal in a 1:1 ratio. Moreover, the optical rotation of 2*H*-pyran **14** is close to 0, which suggests that racemization has taken place at the stage of this intermediate, likely through ring-opening−ring-closure rapid equilibrium and hexadienone helix inversion.[61,62]

The oxiranyl propargylic acetate *syn*-**13**, in contrast, gave a complex mixture containing, at low conversions, both 2*H*-pyran **14** and compound **15**, but the expected final cyclopentenone **16** could not be isolated. This result appears to be an exception to the general behavior described by Sarpong with regard to the stereoconvergency of the process, and its uniqueness must be related to the presence of the sterically congested environment brought by the methyl substituent at the epoxide of substrate **13**. Moreover, the experiment failed to clarify whether the individual diastereomers converge to the final cyclopentenone (*R**,*S**)-**16**.

Puzzled by the different outcome of the diastereomers of substrate **13**, we prepared and treated separatedly under the same reaction conditions the diastereomers of the oxiranyl propargylic acetate that lack the ring methyl groups, which is the substrate previously used for the computations (**iv**), and found that they

dx.doi.org/10.1021/jo301651r | J. Org. Chem. 2012, 77, 8733−8743

Scheme 5. Pt-Catalyzed Rearrangement of Enantiopure Methyl (*R*)- and (*S*)-4-Acetoxy-4-((1*S*,6*S*)-2,2,6-trimethyl-7-oxabicyclo[4.1.0]heptan-1-yl)but-2-ynoate, *anti*-13 and *syn*-13, Respectively, and of Racemates *anti*-i and *syn*-i

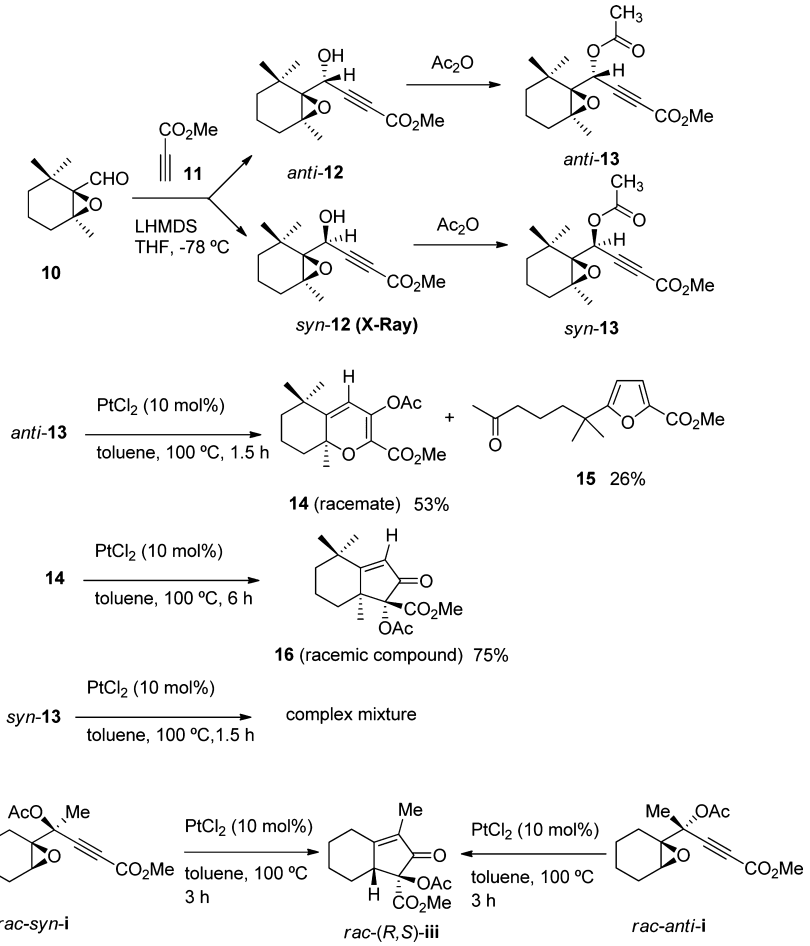

rearranged to the same cyclopentenone (*R**,*S**)-**iii**, as previously described[36] starting from the mixture of diastereomers of **i** (Scheme 5).

Thus, we can conclude that there is no chirality transfer and that the reaction product is a racemic mixture, irrespective of whether the substrate is itself a racemic mixture or an enantiopure compound. We have also determined that the mechanism is stereoconvergent, since both diastereomers (*syn* and *anti*) of the starting product lead to the same (*R**,*S**) cyclopentenone.

The energetic span computed from the data in Table S1 using the *AUTOF* software is 18.1 kcal/mol (see Supporting Information for details). According to this result, heating to 100 °C would then not be required to trigger the reaction. In fact, using epoxyester **13**, we could confirm that the rearrangement takes place already at lower temperatures (40 °C, 24 h), thus bringing computations and experimental predictions into closer agreement.

Computational Insights into the Stereoconvergence of the $PtCl_2$-Catalyzed Rearrangement of Oxiranyl Propargylic Esters. In order to shed light into the stereoconvergence of the reaction, we next carried out a comprehensive study (see Scheme 6) on the rearrangement of acyclic model systems **17** (*syn* and *anti* diastereomers).

The formation of similarly bidentate π complexes between $PtCl_2$ and each diastereomer of **17** (**18** and **18′** for the *syn* and *anti* diastereomers, respectively) leads through 1,2-carboxyl migration via intermediates **19** and **19′** to platinum carbenoids **20** and **20′** with nearly planar structures and T geometries around the metal centers (Figure 1). Their evolution is similar to that of the bicyclic epoxide, and the capture by the oxirane is accompanied by rotation of the platinum to the β face (see Figure S1 for a relaxed scan of the C−O distance starting from **20′** which clearly shows how this conformational change is coupled to the bond-forming process). As a consequence, the *syn* and the *anti* path converge to the same highly congested bicyclic oxonium ion **21**. Compound **21** in turn undergoes a facile (about 3 kcal/mol) fragmentation/ring expansion to afford the platinum-coordinated 2*H*-pyran **22**.

There are noticeable differences in the activation barriers and the relative stabilities of the intermediates found along the pathways for each of the diastereomers. The barrier for the nucleophilic attack of the acetate to the activated alkyne in the rearrangement of *syn*-**18** is larger than that of *anti* diastereomer (**18′**, 15.3 vs 7.7 kcal/mol) and much larger than those determined in similar gold or platinum catalyzed 1,2-acyl migrations (2.4−4.3 kcal/mol).[20,63] This can be explained by the loss of the stabilization associated with the coordination to the oxirane oxygen along this process. In addition, intermediate **19′** is highly destabilized compared to **19** as a consequence of the charge density accumulated due to the proximity of the oxygen and the negatively charged metal fragment which forces the molecule to adopt an unstable half-chair conformation.

dx.doi.org/10.1021/jo301651r | J. Org. Chem. 2012, 77, 8733−8743

Scheme 6. Activation of the Diastereomeric Acetoxy Propargyloxiranes 17 by $PtCl_2$ and Common Transformation into 22[a]

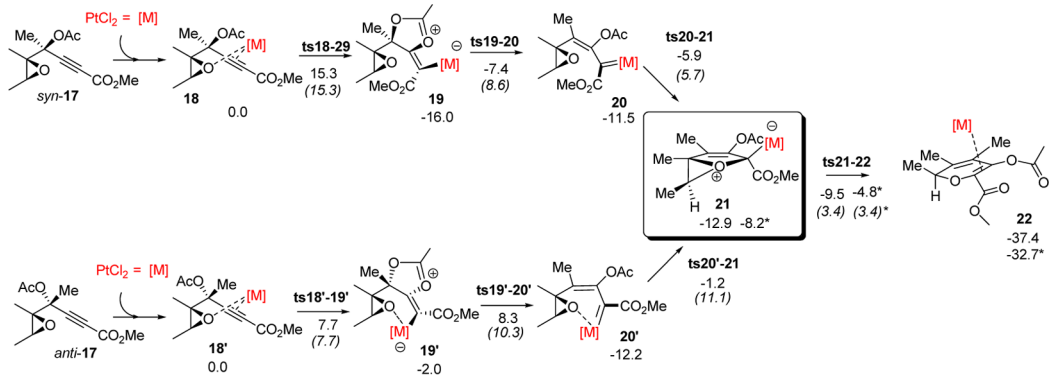

[a]Relative and activation (*in parentheses*) free energies (in kcal/mol) have been computed at the M06/6-31++G(d,p) level in toluene (PCM). Diastereomeric complexes **18** and **18′** have been chosen as the energy reference of the corresponding branch of the mechanism to reinforce that, although isomers, the two starting points are different entities.

Scheme 7. Competing Electrocyclic Ring-Opening-Iso-Nazarov Electrocyclizations Starting from 2*H*-pyran 22[a]

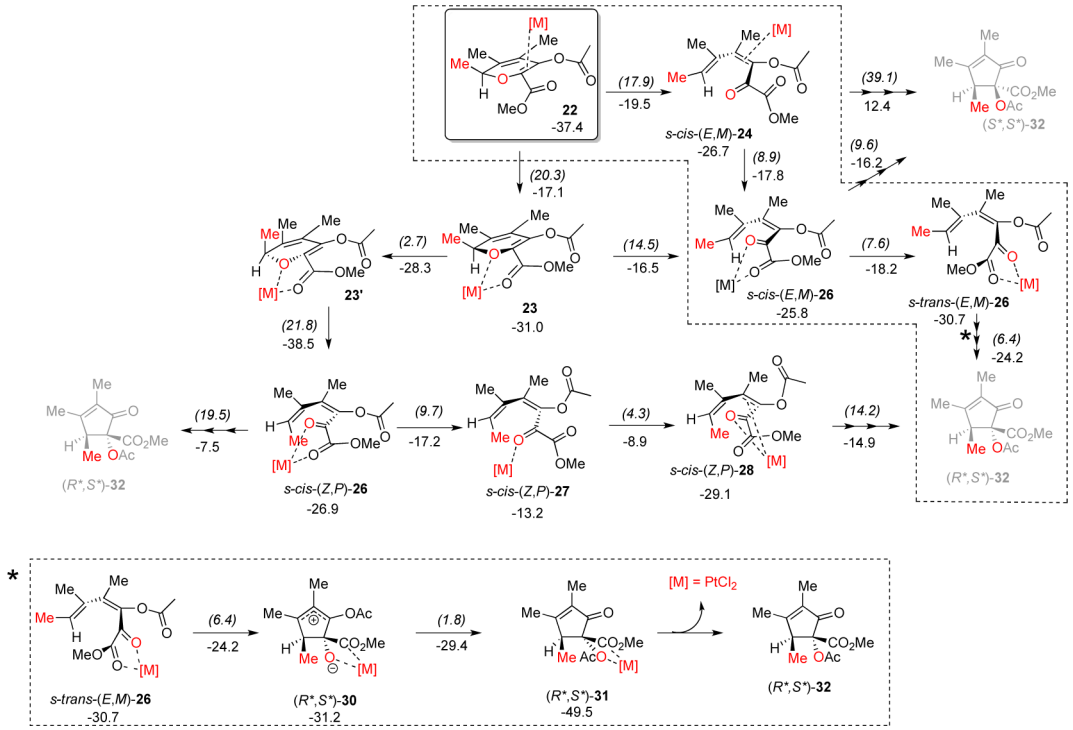

[a]Activation energies (in kcal/mol) have been computed at the M06/6-31++G(d,p) level in toluene (PCM).

Therefore, calculations predict that the first part of the rearrangement is stereoconvergent and the two diastereomers of **17** lead to a single diastereoisomer **22**, which places the metal complexed to the same face of the methyl group. This mechanistic convergence explains why a single product is obtained from a mixture of *syn* and *anti* diastereomers of the acetoxypropargyloxirane **17** (and, by extension, of **i**).

From complex **22**, we have carried out comprehensive computational studies of the different mechanistic manifolds for the rearrangement, in addition to the pathway equivalent to that described for **i** via *s-trans*-(*E,M*)-**26** (Scheme 7). This survey includes the study of other electrocyclic ring-opening processes that could take place from **22** or other haptomers and isomers obtained by a switch of the 2*H*-pyran ring puckering. At an additional level of complexity, we have also considered that the iso-Nazarov electrocyclization proposed for *s-trans*-(*E,M*)-**26** could also occur from structures *s-cis*-(*E,M*)-**26** or from the corresponding (*Z,P*) diastereomers, which are potentially accessible from the same intermediates. In some of these cases, the (*S**,*S**)-**32** diastereomer of the experimentally reported product would be obtained instead of or in addition to the observed (*R**,*S**)-**32**. A selection of the complex manifold of metal migrations and conformational changes that support our mechanistic proposal, together with the corresponding activation free energy values, is summarized in Scheme 7, and a complete picture can be found in the Supporting Information.

To facilitate the perusal of Scheme 7, we have grouped the structures of the intermediates according to the geometry (*Z* or *E*) of the terminal double bond and the helicity (*P* or *M*) of the α-methoxycarbonyl dienone. After the formation of **22**

dx.doi.org/10.1021/jo301651r | J. Org. Chem. 2012, 77, 8733−8743

(the product of the ring expansion of **21**; equivalent to **5** in Scheme 4), two paths are available: a direct ring-opening to afford *s-cis*-(*E,M*)-**24**, or a change of hapticity of the platinum to coordinate the ester and pyran oxygen forming **23**. After **23**, a similar bifurcation would be found leading to either the inverted 2*H*-pyran conformer **23′** (a ring flip that shifts the metal from the β to to the α face) or to the ring-opening product *s-cis*-(*E,M*)-**26**. From **23′**, the ring-opening would produce diastereomer *s-cis*-(*Z,P*)-**26** with an energy of activation of 21.8 kcal/mol. Iso-Nazarov-like cyclizations from *s-cis*-(*E,M*)-**26** and *s-cis*-(*Z,P*)-**26** configurations provide ultimately diastereomeric cyclopentenones (*S**,*S**)-**32** and (*R**,*S**)-**32**, respectively, with energies of activation of 9.6 and 19.5 kcal/mol. Among the paths described up to this moment, the lowest energy corresponds to that leading to *s-cis*-(*E,M*)-**26** (Scheme 7). If this path were followed and the latter species opened directly, the nonobserved (*S**,*S**)-**32** diastereomer would be the predicted product. However, alternatively a conformational change from the *s-cis* to the *s-trans* dienone of *s-cis*-(*E,M*)-**26** would afford *s-trans*-(*E,M*)-**26** which would then cyclize to yield the (*R**,*S**)-**32** diastereomer with an energy cost of 6.4 kcal/mol. Thus, as discussed in the cyclic system, the lowest-energy ring-opening corresponds to the **23** to *s-cis*-(*E,M*)-**26** transformation (14.5 kcal/mol), but we propose a conformational change prior to the ensuing iso-Nazarov reaction in order to minimize the barrier required for this key cyclization (6.4 kcal/mol starting from *s-trans*-(*E,M*)-**26** vs 9.6 kcal/mol starting from *s-cis*-(*E,M*)-**26**). Moreover, as discussed in the cyclic system (an evolution analogous to the **5**-*s-cis*-(*M*)-**7′**-*s-cis*-(*M*)-**7**-*s-trans*-(*M*)-**7** path), the costly formation of **23** can be circumvented by direct ring-opening of **22** to afford *s-cis*-(*E,M*)-**24** and metal migration to generate *s-cis*-(*E,M*)-**26**.

In order to discard the competition of alternative pathways that could erode the diastereoselectivity of the preferred *s-trans*-(*E,M*)-**26** to **30** transformation, we have also explored the iso-Nazarov cyclization step of other platinum complexes (haptomers, diastereomers, and conformers). In the Supporting Information, we provide the activation free energies computed for the electrocyclic ring closure reactions of the relevant dienones, including those corresponding to Scheme 7. The activation energies of these species with alternative mono- and bidentate coordinated platinum complexes and their diastereomers range from 7.9 to 30.0 kcal/mol above that of the favored pathway.

In order to evaluate the role of platinum (if any) after the capture of carbenoids **20** and **20′**, we have also analyzed the steps in this part of the mechanism for the metal free structures, **33** and **33′** (see Scheme 8). We found that Pt coordination to the polyfunctionalized 2*H*-pyran favors the electrocyclic ring-opening reaction in the two cases (with barriers of 21.0 kcal/mol for **33** and 26.8 kcal/mol for **33′**, versus 14.5 and 21.8, kcal/mol for **23** and **23′**, respectively; see Schemes 7 and 8). This involvement of the metal center in the two parts of the mechanism is confirmed with the experimental results of Sarpong et al. who reported, in fact, that heating the 2*H*-pyran intermediate did not produce any reaction in the absence of $PtCl_2$ (in our hands, however, this rearrangement took place upon heating to 160 °C in xylene, compared to the 40 °C needed for the metal-catalyzed reaction). Moreover, our computations predict (see Schemes 7 and 8) that only when the metal coordinates both the pyran heteroatom and the neighboring carboxyl group is the ring-opening accelerated (14.5 kcal/mol for **23** to *s-cis*-(*E,M*)-**26** and 21.8 for **23′** to *s-cis*-(*Z,P*)-**26** vs 21.0 and 26.8 kcal/mol for **33** and **33′**). Similarly to the retroelectrocyclic reaction, the iso-Nazarov reaction is very unlikely to occur from the uncomplexed dienone. The metal promotes this unfavorable reaction through activation of the ketone group, in particular, when in synergy with the complexed vicinal ester carbonyl. For this system (ring closure of *s-trans*-(*E,M*)-**26**, Scheme 8), the electrocyclic reaction shows the lowest activation energy (6.4 kcal/mol) of the series considered. In a sense, the net effect of the metal in *s-trans*-(*E,M*)-**26** is to favor the rearrangement of the oxocarbenium ion and to stabilize the forming alkoxide.

Scheme 8. Electrocyclic Ring-Opening--iso-Nazarov Electrocyclizations in the Absence of the Platinum Catalyst[a]

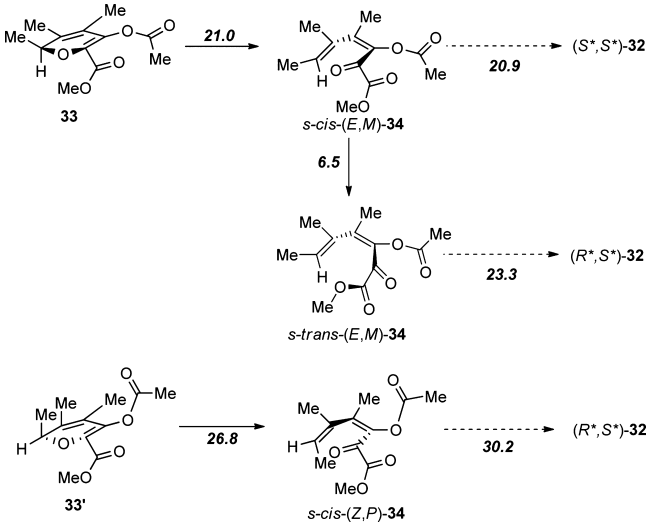

[a]Relative energies and activation energies (in kcal/mol) have been computed at the M06/6-31++G(d,p) level in toluene (PCM).

Relative to their canonical counterparts, these tandem electrocyclic reactions are energetically penalized: we have computed values of 9.4 kcal/mol for the ring-opening of model 2*H*-pyran to dienal[64] (cf., 21.0 and 26.8 kcal/mol for the ring-opening of isomeric 2*H*-pyrans **33** and **33′**, respectively) and of 13.9 kcal/mol for the iso-Nazarov reaction of activated 2,4-pentadienal[55] (20.9 and 30.2 kcal/mol for the iso-Nazarov reaction of *s-cis*-(*E,M*)-**34** and *s-cis*-(*Z,P*)-**34**, respectively; see Scheme 8) using DFT. The high density of functional groups with their conflicting electronic demands in the increasingly polarized structures going from **22** to **32** could be deemed responsible for the rate retardation of these rearrangements.

Thus, we have proposed a mechanism (see Figure 2 for the associated energy profile) for the transformation of epoxy-propargylic esters **i** into cyclopentenones **iii**, which displays some very interesting features: a pair of diastereomers converge to a single product through a delicate balance between the barriers for alternative ring-openings and cyclizations for different haptomers or conformers of the structures of a 2*H*-pyran or dienone intermediates. The configuration of the epoxide determines the configuration of the (*R**,*S**)-**iii** product that is obtained in a chirality transfer process which relies first in the configuration of the stereocenter in **5**/**22** and its coordination to Pt and then in the helicity and *s-cis*/*s-trans* conformation of **7**/**26**, and the torquoselectivity in the subsequent Nazarov reaction that is a consequence of it. The metal center is needed for all the key steps in the mechanism, from the initial 1,2-ester migration to the iso-Nazarov cyclization, changing its function along the reaction path from π-acid to

dx.doi.org/10.1021/jo301651r | J. Org. Chem. 2012, 77, 8733−8743

carbene stabilizer to Lewis acid, and playing an essential role in the chirality transfer process.

CONCLUSIONS

The rearrangement of oxiranyl propargylic acetates induced by substoichiometric quantities of $PtCl_2$ has been revisited with the computational study of cyclic (Figure 2) and acyclic model systems and by the experimental analysis of the reaction course of the enantiopure diastereomers of substrate **13**. We could confirm that the reaction of **13** is stereoconvergent and produces the cyclopentenone (*R**,*S**)-**16** (a racemic mixture in the crystal structure) as the major product and exclusive diastereoisomer. The absolute configuration of the reactant is not preserved in the helical conformations of the intermediate acetoxy dienylketoesters and, therefore, not transferred to the product in this Pt-catalyzed rearrangement, contrary to what is found for other propargylic systems with Au. The complexity of the mechanism for this transformation was revealed computationally and shown to involve the intermediacy of not only the isolated 2*H*-pyran, but also other species. Along the pathways (Figure 2), Pt acts as a multifuncional catalyst: in the first section of the mechanism, the metal appears to donate charge, but in the second section, it withdraws it from the pentadienyl system to favor the iso-Nazarov reaction. Overall, through multiple coordination modes of platinum to the diverse functional groups of the molecule (both oxygen lone pairs and olefins) there is a gradual accumulation of the carbonyl groups (ketone, acetate, and ester) in the same molecular region in the product.

EXPERIMENTAL SECTION

Materials and Methods. Solvents were dried according to published methods and distilled before use. All other reagents were commercial compounds of the highest purity available. Unless otherwise indicated, all reactions were carried out under argon atmosphere in oven-dried glassware. Analytical thin layer chromatography (TLC) was performed on aluminum plates with Kieselgel 60F254 and visualized by UV irradiation (254 nm) or by staining with an ethanolic solution of phosphomolibdic acid. Flash column chromatography was carried out using Kieselgel 60 (230−400 mesh) under pressure. IR spectra were obtained on a spectrophotometer from a thin film deposited onto NaCl glass. Specific rotations were obtained on a polarimeter. For the mass spectra, an FT-ICR MS, equipped with a 7T actively shielded magnet was used and ions were generated using an API electrospray ionization (ESI) source, with a voltage between 1800 and 2200 V (to optimize ionization efficiency) applied to the needle, and a counter voltage of 450 V applied to the capillary. The ESI spectra samples were prepared by adding a spray solution of 70:29.9:0.1 (v/v/v) CH_3OH/water/formic acid to a solution of the sample at a v/v ratio of 1% to 5% to give the best signal-to-noise ratio. High resolution mass spectra were taken on a Autospec instrument. ^1H NMR spectra were recorded in $CDCl_3$ at ambient temperature on a spectrometer at 400 MHz with residual protic solvent as the internal reference [$CDCl_3$, δ_H = 7.26 ppm]; chemical shifts (*d*) are given in parts per million (ppm), and coupling constants (*J*) are given in Hertz (Hz). The proton spectra are reported as follows: δ (multiplicity, coupling constant *J*, number of protons). ^{13}C NMR spectra were recorded in $CDCl_3$ at ambient temperature on the same spectrometer at 100 MHz, with the central peak of $CDCl_3$ (δ_C = 77.16 ppm) as the internal reference. DEPT135 were used to aid in the assignment of signals in the ^{13}C NMR spectra. Additional COSY and HSQC spectra were recorded in particular cases to enable interpretation of ^1H NMR data. Melting points are uncorrected. Crystallographic information was obtained from the corresponding single crystals analyzed by X-ray diffraction. Crystallographic data were collected on a single crystal diffractometer equipped with charge-coupled-device (CCD) detector at 20 °C using graphite monochromated Mo Kα radiation (λ = 0.71073 Å), and were corrected for Lorentz and polarization effects.

Methyl (1′*S*,4*S*,6′*S*)- and (1′*S*,4*R*,6′*S*)-4-Hydroxy-4-(2,2,6-trimethyl-7-oxabicyclo[4.1.0]heptan-1-yl)but-2-ynoate *syn*-12 and *anti*-12. A flame-dried, round-bottom flask was charged with anhydrous THF (2.2 mL) and methyl propiolate **11** (0.315 mL, 3.54 mmol). The solution was cooled down to −78 °C and LiHMDS (3.32 mL, 3.32 mmol, 1.0 M in hexanes) was added slowly. The solution was stirred for 45 min at −78 °C, and then (1*R*,6*S*)-2,2,6-trimethyl-7-oxabicyclo[4.1.0]heptane-1-carbaldehyde **10** (372 mg, 2.22 mmol) was added slowly. The mixture was stirred for 2 h at −78 °C. Then, sat. aqueous NH_4Cl solution was added slowly, and the mixture was left to reach room temperature. The mixture was diluted with Et_2O, and extracted with Et_2O (3×), and the combined organic layers were washed with brine solution (1×) and dried over Na_2SO_4. The solvent was removed under reduced pressure, and the residue was purified by column chromatography on silica gel (gradient from 90:10 to 80:20 hexane/EtOAc) to afford two diastereomers of the corresponding propargylic alcohol (462.6 mg, 83% yield) in a 1.0:1.65 *syn*-**12**/*anti*-**12** ratio.

Data for methyl (1′*R*,4*R*,6′*R*)-4-hydroxy-4-(2,2,6-trimethyl-7-oxabicyclo[4.1.0]heptan-1-yl)but-2-ynoate *syn*-**12**: m.p.: 52−53 °C (hexanes). ^1H NMR (400 MHz, $CDCl_3$): δ 4.82 (s, 1H), 3.77 (s, 3H), 1.9−1.8 (m, 1H), 1.8−1.7 (m, 1H), 1.52 (s, 3H), 1.4−1.3 (m, 3H), 1.2−1.1 (m, 1H), 1.12 (s, 3H), 1.01 (s, 3H) ppm. ^{13}C NMR (100 MHz, $CDCl_3$): δ 153.8 (s), 86.6 (s), 76.7 (s), 70.6 (s), 66.3 (s), 57.5 (d), 52.9 (q), 36.6 (t), 33.3 (s), 31.4 (t), 24.6 (q), 24.4 (q), 21.2 (q), 17.0 (t) ppm. IR (NaCl): ν 3600−3400 (br, OH), 2941 (m, C—H), 2239 (m, C≡C), 1719 (s, C═O), 1436 (w), 1252 (s) cm^{-1}. HRMS (ESI^+): calcd for $C_{14}H_{21}O_4$ ($[M+H]^+$), 253.1434; found, 253.1434. $[\alpha]_D^{24}$ −3.4 (*c* 0.62, MeOH).

Data for (1′*S*,4*S*,6′*S*)-**12**: $[\alpha]_D^{24}$ +3.3 (*c* 1.19, MeOH).

Data for methyl (1′*R*,4*S*,6′*R*)-4-hydroxy-4-(2,2,6-trimethyl-7-oxabicyclo[4.1.0]heptan-1-yl)but-2-ynoate *anti*-**12**: ^1H NMR (400 MHz, $CDCl_3$): δ 4.85 (s, 1H), 3.77 (s, 3H), 1.9−1.8 (m, 1H), 1.8−1.7 (m, 1H), 1.48 (s, 3H), 1.4−1.2 (m, 3H), 1.30 (s, 3H), 1.1−1.0 (m, 1H), 1.1 (s, 3H) ppm. ^{13}C NMR (100 MHz, $CDCl_3$): δ 153.9 (s), 85.6 (s), 79.4 (s), 70.1 (s), 66.1 (d), 64.3 (s), 52.9 (q), 38.5 (t), 33.8 (s), 32.1 (t), 26.0 (q), 25.9 (q), 21.4 (q), 17.0 (t) ppm. IR (NaCl): ν 3600−3400 (br, OH), 2941 (m, C—H), 2236 (m, C≡C), 1718 (s, C═O), 1436 (w), 1252 (s) cm^{-1}. HRMS (ESI^+): calcd for $C_{14}H_{21}O_4$ ($[M+H]^+$), 253.1434; found, 253.1427. $[\alpha]_D^{22}$ −9.9 (*c* 1.31, MeOH).

Data for (1′*S*,4*R*,6′*S*)-**12**: $[\alpha]_D^{26}$ +10.0 (*c* 1.09, MeOH).

Methyl (1′*S*,4*S*,6′*S*)-4-Acetoxy-4-(2,2,6-trimethyl-7-oxabicyclo[4.1.0]heptan-1-yl)but-2-ynoate *syn*-13. To a solution of methyl (1′*S*,4*S*,6′*S*)-4-hydroxy-4-(2,2,6-trimethyl-7-oxabicyclo-[4.1.0]heptan-1-yl)but-2-ynoate *syn*-**12** (81.5 mg, 0.323 mmol) in anhydrous methylene chloride (2 mL) were added triethylamine (134 μL, 0.97 mmol), acetic anhydride (38 μL, 0.40 mmol), and DMAP (3.9 mg, 0.03 mmol) at 23 °C. The resultant mixture was stirred for 1.5 h, then washed with 1% aqueous HCl solution (2×) and brine (1×), dried over Na_2SO_4, and the solvent was removed under reduced pressure. The residue was purified by column chromatography on silica gel (gradient from 95:5 to 80:20 hexane/EtOAc) to afford 85.5 mg (90%) of a colorless oil identified as methyl (1′*S*,4*S*,6′*S*)-4-acetoxy-4-(2,2,6-trimethyl-7-oxabicyclo[4.1.0]heptan-1-yl)but-2-ynoate *syn*-**13**.

^1H NMR (400 MHz, $CDCl_3$): δ 5.87 (s, 1H), 3.78 (s, 3H), 2.07 (s, 3H), 1.9−1.8 (m, 1H), 1.8−1.7 (m, 1H), 1.44 (s, 3H), 1.4−1.3 (m, 3H), 1.19 (s, 3H), 1.11 (s, 3H), 1.1−1.0 (m, 1H) ppm. ^{13}C NMR (100 MHz, $CDCl_3$): δ 168.7 (s), 153.4 (s), 83.4 (s), 78.1 (s), 68.5 (s), 63.7 (s), 60.4 (d), 53.0 (q), 37.6 (t), 33.6 (s), 31.9 (t), 25.6 (q), 24.9 (q), 20.7 (q), 20.4 (q), 17.0 (t) ppm. IR (NaCl): ν 2942 (m, C−H), 2247 (m, C≡C), 1755 (s, C═O), 1721 (s, C═O), 1436 (w), 1370 (w), 1256 (s), 1220 (s) cm^{-1}. HRMS (ESI^+): calcd for $C_{16}H_{23}O_5$ ($[M+H]^+$), 295.1540; found, 295.1536. $[\alpha]_D^{24}$ 26.7 (*c* 1.06, MeOH).

Data for (1′*R*,4*R*,6′*R*)-**13**: $[\alpha]_D^{24}$ −27.2 (*c* 1.20, MeOH).

Methyl (1′*S*,4*R*,6′*S*)-4-Acetoxy-4-(2,2,6-trimethyl-7-oxabicyclo[4.1.0]heptan-1-yl)but-2-ynoate *anti*-13. To a solution of (1′*S*,4*R*,6′*S*)-methyl 4-hydroxy-4-(2,2,6-trimethyl-7-oxabicyclo-[4.1.0]heptan-1-yl)but-2-ynoate *anti*-**12** (174 mg, 0.69 mmol) in

dx.doi.org/10.1021/jo301651r | J. Org. Chem. 2012, 77, 8733−8743

anhydrous methylene chloride (4.2 mL) were added triethylamine (287 μL, 2.07 mmol), acetic anhydride (81 μL, 0.86 mmol), and DMAP (8.4 mg, 0.07 mmol) at 23 °C. The resultant mixture was stirred for 1.5 h, then washed with 1% aqueous HCl solution (2×) and brine (1×), dried over Na_2SO_4, and the solvent was removed under reduced pressure. The residue was purified by column chromatography on silica gel (gradient from 95:5 to 80:20 hexane/EtOAc) to afford 158.1 mg (78%) of a white solid identified as methyl (1′*S*,4*R*,6′*S*)-4-acetoxy-4-(2,2,6-trimethyl-7-oxabicyclo[4.1.0]heptan-1-yl)but-2-ynoate *anti*-**13**. ^{1}H NMR (400 MHz, $CDCl_3$): δ 5.74 (s, 1H), 3.74 (s, 3H), 2.11 (s, 3H), 1.9−1.8 (m, 1H), 1.8−1.7 (m, 1H), 1.49 (s, 3H), 1.4−1.3 (m, 3H), 1.15 (s, 3H), 1.06 (s, 3H), 1.1−1.0 (m, 1H) ppm. ^{13}C NMR (100 MHz, $CDCl_3$): δ 169.1 (s), 153.4 (s), 82.1 (s), 79.5 (s), 68.3 (s), 66.2 (d), 64.2 (s), 52.9 (q), 38.0 (t), 34.0 (s), 31.7 (t), 25.5 (q, 2×), 21.5 (q), 20.9 (q), 16.9 (t) ppm. IR (NaCl): ν 2949 (m, C—H), 2243 (m, C≡C), 1755 (s, C═O), 1720 (s, C═O), 1436 (w), 1370 (w), 1258 (s), 1217 (s) cm^{-1}. HRMS (ESI$^+$): calcd for $C_{16}H_{23}O_5$ ([M+H]$^+$), 295.1540; found, 295.1543. $[\alpha]_D^{23}$ −27.3 (*c* 1.12, MeOH).

Data for (1′*R*,4*S*,6′*R*)-**13**: $[\alpha]_D^{22}$ 28.0 (*c* 0.79, MeOH).

***rac*-Methyl 3-Acetoxy-5,5,8a-trimethyl-6,7,8,8a-tetrahydro-5*H*-chromene-2-carboxylate 14.** A flame-dried 25 mL Schlenk flask equipped with a Teflon screw-top cap was charged with (1′*S*,4*R*,6′*S*)-methyl 4-acetoxy-4-(2,2,6-trimethyl-7-oxabicyclo[4.1.0]-heptan-1-yl)but-2-ynoate *anti*-**13** (67.3 mg, 0.229 mmol) and $PtCl_2$ (0.6 mg, 0.002 mmol) in anhydrous toluene (1.15 mL). The mixture was flushed with argon by sparging over 1 min and capped tightly. The flask was placed in an oil bath at 100 °C and held at this temperature for 1.5 h. At the completion of the reaction, the solvent was removed by evaporation under reduced pressure, and the residue was purified by column chromatography on silica gel (gradient from 95:5 to 80:20 hexane/EtOAc) to afford 35.8 mg (53%) of a colorless oil identified as *rac*-methyl 3-acetoxy-5,5,8a-trimethyl-6,7,8,8a-tetrahydro-5*H*-chromene-2-carboxylate **14** accompanied by 15.0 mg (26%) of a colorless oil identified as methyl 5-(2-methyl-6-oxoheptan-2-yl)furan-2-carboxylate **15** as a side product. ^{1}H NMR (400 MHz, $CDCl_3$): δ 5.68 (s, 1H), 3.76 (s, 3H), 2.24 (s, 3H), 2.14 (d, *J* = 12.8 Hz, 1H), 1.87 (td, *J* = 13.5, 4.4 Hz, 1H), 1.68 (tt, *J* = 14.0, 3.9 Hz, 1H), 1.6−1.5 (m, 1H), 1.49 (s, 3H), 1.5−1.4 (m, 1H), 1.38 (dd, *J* = 12.9, 4.0 Hz, 1H), 1.17 (s, 3H), 1.12 (s, 3H) ppm. ^{13}C NMR (100 MHz, $CDCl_3$): δ 169.1 (s), 162.2 (s), 152.5 (s), 140.4 (s), 130.5 (s), 114.6 (d), 79.2 (s), 52.0 (q), 39.5 (t), 38.6 (t), 35.9 (s), 30.7 (q), 30.1 (q), 23.3 (q), 20.8 (q), 18.8 (t) ppm. IR (NaCl): ν 2947 (m, C—H), 1772 (s, C═O), 1719 (s, C═O), 1193 (s, C−O−C) cm^{-1}; HRMS (ESI$^+$): calcd for $C_{16}H_{23}O_5$ ([M+H]$^+$), 295.1540; found: 295.1541.

Data for methyl 5-(2-methyl-6-oxoheptan-2-yl)furan-2-carboxylate **15**: ^{1}H NMR (400 MHz, $CDCl_3$): δ 7.07 (d, *J* = 3.4 Hz, 1H), 6.12 (d, *J* = 3.4 Hz, 1H), 3.86 (s, 3H), 2.36 (t, *J* = 7.3 Hz, 2H), 2.09 (s, 3H), 1.64−1.57 (m, 2H), 1.44−1.37 (m, 2H), 1.29 (s, 6H) ppm. ^{13}C NMR (100 MHz, $CDCl_3$): δ 209.0 (s), 167.6 (s), 159.5 (s), 143.0 (s), 119.1 (d), 106.4 (d), 51.8 (q), 44.0 (t), 41.2 (t), 36.4 (s), 30.0 (q), 26.7 (q, 2×), 19.1 (t) ppm. IR (NaCl): ν 2962 (m, C—H), 1732 (s, C═O), 1715 (s, C═O), 1519 (m), 1306 (s), 1137 (m, C−O−C) cm^{-1}. HRMS (ESI$^+$): calcd for $C_{14}H_{21}O_4$ ([M+H]$^+$), 253.14344; found: 253.14271.

Methyl (1*R,7a*S**)-1-Acetoxy-4,4,7a-trimethyl-2-oxo-2,4,5,6,7,7a-hexahydro-1*H*-indene-1-carboxylate 16.** A flame-dried 25 mL Schlenk flask equipped with a Teflon screw-top cap was charged with *rac*-methyl 3-acetoxy-5,5,8a-trimethyl-6,7,8,8a-tetrahydro-5*H*-chromene-2-carboxylate **14** (21.0 mg, 0.071 mmol) and $PtCl_2$ (0.2.0 mg, 0.007 mmol) in anhydrous toluene (0.4 mL). The mixture was flushed with argon by sparging over 1 min and capped tightly. The flask was placed in an oil bath at 100 °C and held at this temperature for 7 h. At the completion of the reaction, the solvent was removed by evaporation under reduced pressure and the residue was purified by flash chromatography on silica gel (gradient from 85:15 to 80:20 hexane/EtOAc) to afford 16.7 mg (79%) of a white solid identified as the racemic mixture of (1*R**,7a*S**)-methyl 1-acetoxy-4,4,7a-trimethyl-2-oxo-2,4,5,6,7,7a-hexahydro-1*H*-indene-1-carboxylate **16**. The composition of *rac*-**16** (t_R = 24.0 and 32.6 min) as a 50:50 mixture of enantiomers was determined using chiral HPLC (Chiralpak IA, 250 × 10 mm, 65:35 hexane/*t*-BuOMe, 3.0 mL/min, detection at 230 nm). m.p.: 95−96 °C (hexane/Et_2O). ^{1}H NMR (400 MHz, $CDCl_3$): δ 5.99 (s, 1H), 3.69 (s, 3H), 2.21 (s, 3H), 2.1−1.9 (m, 1H), 1.9−1.7 (m, 2H), 1.7−1.5 (m, 3H), 1.27 (s, 6H), 1.24 (s, 3H) ppm. ^{13}C NMR (100 MHz, $CDCl_3$): δ 197.1 (s), 193.4 (s), 169.8 (s), 166.2 (s), 123.4 (d), 92.7 (s), 52.9 (q), 51.6 (s), 39.0 (t), 36.3 (s), 33.5 (t), 31.1 (q), 29.0 (q), 26.2 (q), 21.0 (q), 18.5 (t) ppm. IR (NaCl): ν 2950 (m, C—H), 1749 (s, C═O), 1722 (s, C═O), 1237 (s, C−O−C) cm^{-1}; HRMS (ESI$^+$): *m*/*z* calcd for $C_{16}H_{23}O_5$ ([M+H]$^+$), 295.15400; found, 295.15501.

Following the same procedure, starting from methyl (1′*S*,4*R*,6′*S*)-4-acetoxy-4-(2,2,6-trimethyl-7-oxabicyclo[4.1.0]heptan-1-yl)but-2-ynoate *anti*-**13** (91.6 mg, 0.311 mmol) and $PtCl_2$ (0.8 mg, 0.003 mmol) in anhydrous toluene (1.5 mL) after 9 h at 100 °C and purification by flash chromatography on silica gel (gradient from 85:15 to 80:20 hexane/EtOAc) it was obtained 7.9 mg (9%) of *rac*-methyl 3-acetoxy-5,5,8a-trimethyl-6,7,8,8a-tetrahydro-5*H*-chromene-2-carboxylate **14**, 24 mg (26%) of (1*R**,7a*S**)-methyl 1-acetoxy-4,4,7a-trimethyl-2-oxo-2,4,5,6,7,7a-hexahydro-1*H*-indene-1-carboxylate **16**, and 12 mg (15%) of methyl 5-(2-methyl-6-oxoheptan-2-yl)furan-2-carboxylate **15**.

Crystal Structure Data. CCDC 873045 (product **16**) and CCDC 873046 (*syn*-**12**) contains the supplementary crystallographic data for this paper. These data can be obtained free of charge from The Cambridge Crystallographic Data Centre via www.ccdc.cam.ac.uk/data_request/cif.

■ ASSOCIATED CONTENT

Ⓢ Supporting Information

Mechanistic interpretation for the obtention of **15**, crystal structure data for *syn*-**12** and **16**, additional computational data, and reproduction of NMR spectra. This material is available free of charge via the Internet at http://pubs.acs.org/.

■ AUTHOR INFORMATION

Corresponding Author

*E-mail: faza@uvigo.es, qolera@uvigo.es

Notes

The authors declare no competing financial interest.

■ ACKNOWLEDGMENTS

This work was partially supported by grants from the European Union (EPITRON, LSHC-CT2005-518417), MICINN-Spain (SAF2010-17935-FEDER), Xunta de Galicia (INBIOMED, Parga Pondal Contract to B.V.) and the Ramón Areces Foundation (AGP Fellowship). We thank the Centro de Supercomputación de Galicia (CESGA) for generous allocation of computing resources.

■ REFERENCES

(1) Hashmi, A. S. K. *Angew. Chem., Int. Ed.* **2010**, *49*, 5232−5241.
(2) Shapiro, N. D.; Toste, F. D. *Synlett* **2010**, 675−691.
(3) Wang, S.; Zhang, G.; Zhang, L. *Synlett* **2010**, 692−706.
(4) Soriano, E.; Marco-Contelles, J. A. *Acc. Chem. Res.* **2009**, *42*, 1026−1036.
(5) Fürstner, A. *Chem. Soc. Rev.* **2009**, *38*, 3208−3221.
(6) Jiménez-Nuñez, E.; Echavarren, A. M. *Chem. Rev.* **2008**, *108*, 3326−3350.
(7) Widenhoefer, R. A. *Chem.—Eur. J.* **2008**, *14*, 5382−5391.
(8) Skouta, R.; Li, C.-J. *Tetrahedron* **2008**, *64*, 4917−4938.
(9) Shen, H. C. *Tetrahedron* **2008**, *64*, 7847−7870.
(10) Shen, H. C. *Tetrahedron* **2008**, *64*, 3885−3903.
(11) Li, Z.; Brouwer, C.; He, C. *Chem. Rev.* **2008**, *108*, 3239−3265.
(12) Hashmi, A. S. K.; Rudolph, M. *Chem. Soc. Rev.* **2008**, *37*, 1766−1775.

(13) Fürstner, A.; Davies, P. W. *Angew. Chem., Int. Ed.* **2007**, *46*, 3410−3449.
(14) Echavarren, A. M. Molecular diversity through gold catalysis with alkynes. *Chem. Commun.* **2007**, 333−346.
(15) Nieto-Faza, O.; de Lera, A. R. DFT-Based Mechanistic Insights into Noble Metal-Catalyzed Rearrangement of Propargylic Derivatives: Chirality Transfer Processes. In *Computational Mechanisms of Au and Pt Catalyzed Reactions*, Soriano, E., Marco-Contelles, J., Eds.; Springer: Berlin/Heidelberg, 2011; Vol. *302*, pp 81−130.
(16) Toullec, P.; Michelet, V. R. Cycloisomerization of 1,n-Enynes Via Carbophilic Activation. In *Computational Mechanisms of Au and Pt Catalyzed Reactions*, Soriano, E., Marco-Contelles, J., Eds.; Springer: Berlin/Heidelberg, 2011; Vol. *302*, pp 31−80.
(17) Michelet, V.; Toullec, P. Y.; Genêt, J.-P. *Angew. Chem., Int. Ed.* **2008**, *47*, 4268−4315.
(18) Marion, N.; Nolan, S. P. *Angew. Chem., Int. Ed.* **2007**, *46*, 2750−2752.
(19) Fürstner, A.; Hannen, P. *Chem.—Eur. J.* **2006**, *12*, 3006−3019.
(20) Correa, A.; Marion, N.; Fensterbank, L.; Malacria, M.; Nolan, S. P.; Cavallo, L. *Angew. Chem., Int. Ed.* **2008**, *47*, 718−721.
(21) Nieto-Faza, O.; Silva-López, C.; Álvarez, R.; de Lera, A. R. *J. Am. Chem. Soc.* **2006**, *128*, 2434−2437.
(22) Marco-Contelles, J. L.; Soriano, E. *THEOCHEM* **2006**, *761*, 2434−2437.
(23) Soriano, E.; Ballesteros, P.; Marco-Contelles, J. L. *Organometallics* **2005**, *24*, 3172−3181.
(24) Soriano, E.; Ballesteros, P.; Marco-Contelles, J. L. *Organometallics* **2005**, *24*, 3182−3191.
(25) Soriano, E.; Marco-Contelles, J. L. *J. Org. Chem.* **2005**, *70*, 9345−9353.
(26) Soriano, E.; Marco-Contelles, J. Structure, Bonding, and Reactivity of Reactant Complexes and Key Intermediates. In *Computational Mechanisms of Au and Pt Catalyzed Reactions*, Soriano, E., Marco-Contelles, J., Eds.; Springer: Berlin/Heidelberg, 2011; Vol. *302*, pp 1−29.
(27) Benitez, D.; Shapiro, N. D.; Tkatchouk, E.; Wang, Y.; Goddard, W. A.; Toste, F. D. *Nat. Chem.* **2009**, *1*, 482−486.
(28) Seidel, G.; Mynott, R.; Fürstner, A. *Angew. Chem., Int. Ed.* **2009**, *48*, 2510−2513.
(29) Fürstner, A.; Morency, L. *Angew. Chem., Int. Ed.* **2008**, *47*, 5030−5033.
(30) Zhang, L.; Sun, J.; Kozmin, S. A. *Adv. Synth. Catal.* **2006**, *348*, 2271−2296.
(31) Aubert, C.; Buisine, O.; Malacria, M. *Chem. Rev.* **2002**, *102*, 813−834.
(32) Pérez-Galan, P.; Herrero-Gómez, E.; Hog, D. T.; Martin, N. J. A.; Maseras, F.; Echavarren, A. M. *Chem. Sci.* **2011**, *2*, 141−149.
(33) Cordonnier, M.-C.; Blanc, A.; Pale, P. *Org. Lett.* **2008**, *10*, 1569−1572.
(34) Kern, N.; Blanc, A.; Weibel, J.-M.; Pale, P. *Chem. Commun.* **2011**, *47*, 6665−6667.
(35) Motamed, M.; Bunnelle, E. M.; Singaram, S. W.; Sarpong, R. *Org. Lett.* **2007**, *9*, 2167−2170.
(36) Pujanauski, B. G.; Bhanu Prasad, B. A.; Sarpong, R. *J. Am. Chem. Soc.* **2006**, *128*, 6786−6787.
(37) González Pérez, A.; Silva López, C.; Marco-Contelles, J.; Nieto Faza, O.; Soriano, E.; de Lera, A. R. *J. Org. Chem.* **2009**, *74*, 2982−2991.
(38) Faza, O. N.; López, C. S.; de Lera, A. R. *J. Org. Chem.* **2011**, *76*, 3791−3796.
(39) Zhao, Y.; Truhlar, D. G. *Acc. Chem. Res.* **2008**, *41*, 157−167.
(40) Cramer, C.; Truhlar, D. *Phys. Chem. Chem. Phys.* **2009**, *11*, 10757−10816.
(41) Nieto-Faza, O.; Rodríguez, R.; Silva-López, C. *Theor. Chem. Acc.* **2011**, *128*, 647−661.
(42) Frisch, M. J.; Trucks, G. W.; Schlegel, H. B.; Scuseria, G. E.; Robb, M. A.; Cheeseman, J. R.; Scalmani, G.; Barone, V.; Mennucci, B.; Petersson, G. A.; Nakatsuji, H.; Caricato, M.; Li, X.; Hratchian, H. P.; Izmaylov, A. F.; Bloino, J.; Zheng, G.; Sonnenberg, J. L.; Hada, M.; Ehara, M.; Toyota, K.; Fukuda, R.; Hasegawa, J.; Ishida, M.; Nakajima, T.; Honda, Y.; Kitao, O.; Nakai, H.; Vreven, T.; Montgomery, J. A.; , Jr., Peralta, J. E.; Ogliaro, F.; Bearpark, M.; Heyd, J. J.; Brothers, E.; Kudin, K. N.; Staroverov, V. N.; Kobayashi, R.; Normand, J.; Raghavachari, K.; Rendell, A.; Burant, J. C.; Iyengar, S. S.; Tomasi, J.; Cossi, M.; Rega, N.; Millam, J. M.; Klene, M.; Knox, J. E.; Cross, J. B.; Bakken, V.; Adamo, C.; Jaramillo, J.; Gomperts, R.; Stratmann, R. E.; Yazyev, O.; Austin, A. J.; Cammi, R.; Pomelli, C.; Ochterski, J. W.; Martin, R. L.; Morokuma, K.; Zakrzewski, V. G.; Voth, G. A.; Salvador, P.; Dannenberg, J. J.; Dapprich, S.; Daniels, A. D.; Ö. Farkas, Foresman, J. B.; Ortiz, J. V.; Cioslowski, J.; Fox, D. J. *Gaussian 09, revision A.1*; Gaussian, Inc.: Wallingford, CT, 2009.
(43) Hay, P. J.; Wadt, W. R. *J. Chem. Phys.* **1985**, *82*, 270−283.
(44) Gonzalez, C.; Schlegel, H. B. *J. Phys. Chem.* **1990**, *94*, 5523−5527.
(45) Tomasi, J.; Persico, M. *Chem. Rev.* **1994**, *94*, 2027−2094.
(46) Tomasi, J.; Mennucci, B.; Cammi, R. *Chem. Rev.* **2005**, *105*, 2999−3094.
(47) Kozuch, S.; Shaik, S. *J. Am. Chem. Soc.* **2006**, *128*, 3355−3365.
(48) Kozuch, S.; Shaik, S. *Acc. Chem. Res.* **2010**, *44*, 101−110.
(49) Uhe, A.; Kozuch, S.; Shaik, S. *J. Comput. Chem.* **2011**, *32*, 978−985.
(50) Legault, C. Y. *CYLView, 1.0b*; Université de Sherbrooke: Montreal, Québec, Canada, 2009.
(51) Zhao, H.; Hsu, D. C.; Carlier, P. R. *Synthesis* **2005**, 1−16.
(52) Hu, J. J.; Li, F.; Hor, T. S. A. *Organometallics* **2009**, *28*, 1212−1220.
(53) Fantasia, S.; Petersen, J. L.; Jacobsen, H.; Cavallo, L.; Nolan, S. P. *Organometallics* **2007**, *26*, 5880−5889.
(54) Geng, Z.; Yan, P.; Wang, Y.; Yao, X.; Han, Y.; Liang, J. *J. Phys. Chem. A* **2007**, *111*, 9961−9968.
(55) Nieto-Faza, O.; Silva-López, C.; Álvarez, R.; de Lera, A. R. *Chem.—Eur. J.* **2004**, *10*, 4324−4333.
(56) Nieto-Faza, O.; Silva-López, C.; Alvarez, R.; de Lera, A. R. *Chem.—Eur. J* **2009**, *15*, 1944−1956.
(57) Lin, G.-Y.; Li, C.-W.; Hung, S.-H.; Liu, R.-S. *Org. Lett.* **2008**, *10*, 5059−5062.
(58) Lin, C.-C.; Teng, T.-M.; Tsai, C.-C.; Liao, H.-Y.; Liu, R.-S. *J. Am. Chem. Soc.* **2008**, *130*, 16417−16423.
(59) Bhunia, S.; Liu, R.-S. *J. Am. Chem. Soc.* **2008**, *130*, 16488−16489.
(60) Vaz, B.; Domínguez, M.; Álvarez, A.; de Lera, A. R. *Chem.—Eur. J.* **2007**, *13*, 1273−1290.
(61) Schiess, P.; Seeger, R.; Suter, C. *Helv. Chim. Acta* **1970**, *53*, 1713−1722.
(62) Schiess, P.; Chia, H. L. *Helv. Chim. Acta* **1970**, *53*, 485−495.
(63) Marion, N.; LemiËre, G.; Correa, A.; Costabile, C.; Ramón, R. S.; Moreau, X.; de Frèmont, P.; Dahmane, R.; Hours, A.; Lesage, D.; Tabet, J.-C.; Goddard, J.-P.; Gandon, V.; Cavallo, L.; Fensterbank, L.; Malacria, M.; Nolan, S. P. *Chem.—Eur. J.* **2009**, *15*, 3243−3260.
(64) Silva López, C.; Álvarez, R.; Domínguez, M.; Nieto Faza, O.; de Lera, A. R. *J. Org. Chem.* **2009**, *74*, 1007−1013.